Available online at www.sciencedirect.com
ScienceDirect
Journal of Sound and Vibration 303 (2007) 405–427
JOURNAL OF SOUND AND VIBRATION
www.elsevier.com/locate/jsvi

State sensitivity analysis of the pantograph system for a high-speed rail vehicle considering span length and static uplift force

Jin-Woo Kim[a,*], Ho-Chol Chae[b], Bum-Seok Park[c], Seung-Yeol Lee[d], Chang-Soo Han[d], Jin-Hee Jang[e]

[a]*Department of Mechatronics Engineering, Hanyang University, Sa 1 dong, Sangrok gu, Ansan, Kyonggi Do, 426-791, South Korea*
[b]*Korea FA R&D Center/Display System Institute SFA Engineering Co. 691, Joong-Ri, Dongtan-Myoun, Hwangsung-City, Kyoungki-Do, 445-813, South Korea*
[c]*Department of Precision Mechanical Engineering, Hanyang University,17, Haengdang-dong, Seongdong-gu, Seoul, 133-791, Korea*
[d]*Department of Mechanical Engineering, Hanyang University, 17, Haengdang-dong, Seongdong-gu, Seoul, 133-791, Korea*
[e]*Chassis Development Team Technical Center, GM DAEWOO 199-1, CheongCheon-Dong, Bupyung-Gu, Incheon 403-714, Korea*

Received 13 April 2004; received in revised form 24 August 2005; accepted 12 June 2006

Abstract

In this paper, dynamic characteristics analysis of catenary and pantograph systems for a high-speed rail vehicle is carried out. The catenary system is considered to be a beam model. The analysis of the catenary based on the finite element method (FEM) is performed to develop the pantograph. The stiffness value can be obtained at each nodal point on the contact wire. State sensitivity analysis was executed with respect to design variables considered by the pantograph system. The pantograph of linear spring–mass–damper system is considered as a 3dof model using lumped parameters. Dynamic modeling of the pantograph system is verified by actual experimental vibration data. To perform the sensitivity analysis, our study was considered lift force effect of the pan-head occurring at high-speed runs. Also, a span length and static uplift force were included into design variables. As a result, we could confirm that span length and plunger spring constant are some of the important design variables of catenary and the pantograph systems.

1. Introduction

At present, the high-speed railway that is the next generation of transportation system is characterized by high stability, high driving velocity, and ride comfort as compared to the other transportation systems. An accompanying problem of the high speed of the railway is ensuring stable current collection. For stable operation of a railway, the catenary must be supplied with stable electrical power through solid contact with the pantograph. When the railway speed is increased, contact loss will occur between the pantograph and the catenary due to the catenary stiffness. In addition, wear on the pantograph is going to grow as electrical shock and damage may occur [1]. Therefore, research into understanding the current-collecting system's dynamic

*Corresponding author. Tel.: +82 31 400 4062; fax: +82 31 406 6398.
E-mail addresses: jwkim@krri.re.k (J.-W. Kim), hcchae@sfa.co.kr (H.-C. Chae), bspark@hanyang.ac.kr (B.-S. Park), suprasy@paran.com (S.-Y. Lee), cshan@hanyang.ac.kr (C.-S. Han), gyuhapa@empal.com (J.-H. Jang).

0022-460X/$ - see front matter © 2006 Elsevier Ltd. All rights reserved.
doi:10.1016/j.jsv.2006.06.073

Nomenclature

m_1	mass of the pantograph frame
m_2	mass of the pantograph plunger
m_3	mass of the pantograph pan-head
c_1	damping coefficient between the vehicle body and the frame
c_2	damping coefficient between the frame and the plunger
c_3	damping coefficient between the plunger and the pan-head
k_1	stiffness coefficient between the vehicle body and the pantograph frame
k_2	stiffness coefficient between the frame and the plunger
k_3	stiffness coefficient between the plunger and the pan-head
L	a span length
F_1, F_2, F_3	static uplift force of the pantograph
F_{L1}, F_{L2}, F_{L3}	lift force
y_1	vertical displacement of the upper and lower arm
y_2	vertical displacement of the crossbar and plunger
y_3	vertical displacement of the pan-head
d_1^e, d_3^e	vertical displacement of the contact wire and the messenger wire
d_2^e, d_4^e	angle of rotation of the contact wire and the messenger wire
h	length of one finite element of the wire
K_{ew}	element stiffness matrix of the contact wire and the messenger wire
K_{ed}	element stiffness matrix of the dropper
K_{eb}	element stiffness matrix of the moving bracket
K_{ea}	element stiffness matrix of the steady arm
K	overall stiffness matrix of the catenary
$\underline{d}$	displacement vector of the contact wire
$\underline{f}$	force vector on the contact wire
$\underline{k}$	stiffness vector of the catenary
x	horizontal position in the catenary span

characteristics and the decreasing width of dynamic variation are needed. Progress has been made in recent research assuring the ability of high-speed driving as the basic technology of a high-speed railway [2]. The dynamic interaction of catenary and pantograph systems has been investigated extensively. Ockendon and Taylor [3] described an approximate analytical formulation to determine contact force between a contact wire and a pantograph. Manabe [4] conducted research on wave analyses to study the response between the pantograph and the catenary with discrete support springs. Wu and Brennan [5] investigated the dynamic relation between the catenary and the pantograph using finite element method (FEM). Vinayagalingam [6] studied contact force variation and pan-head trajectory by using finite difference methods. Today's situation is that an active pantograph is proposed for more stable current collection through maximizing the ability of the pantograph to follow the catenary [7–9].

To improve the performance of the pantograph, its dynamics should be considered more precisely before applying an active system. Especially, many researchers trying to improve the system performance, have suggested using sensitivity analysis as an efficient tool for checking variations in design variables based on its dynamics. Vanderplaats and Arora [10,11] found that sensitivity information can be used as a design basis when re-designing a system. Haug et al. [3] investigated dynamic sensitivity analysis which is utilized for variation evaluation of mechanisms in the dynamic state. Jang and Han [12] devised a way to conduct dynamic sensitivity analysis for studying state sensitivity information with respect to changes in design variables. Sensitivity analysis about the pantograph system can be a useful tool to improve dynamic characteristics of a pantograph.

In this study, the dynamic characteristics of a catenary system and pantograph supplying electrical power to high-speed trains are investigated. The analytical model of a catenary and a pantograph is composed to simulate the behavior of an actual system. To obtain the model of the catenary system for high-speed operation, we perform the analysis of the catenary system using FEM. The pantograph system is assumed to be a 3dof model using lumped parameters. The reliability of the dynamic model is verified by the comparison of the excitation test with fast Fourier transform (FFT) of the actual system. State sensitivity analysis was executed with respect to design variables of the pantograph system. Uplift force increased by aerodynamic lift force affects displacement and contact forces occurring in between the catenary and the pantograph system directly. Therefore, the lift force data acquired from experiments are utilized for sensitivity analysis. From

results of the sensitivity analysis, it is established that design variable is more significant for dynamic characteristics of pan-head at high speed.

2. Modeling of the catenary and the pantograph system

2.1. Finite element analysis of the catenary system

2.1.1. Components of the catenary system

A catenary system is an equipment installed overhead in order to supply electric power to a high-speed rail vehicle and consists of contact wire, messenger wire, droppers, moving brackets and steady arms. Contact wire is electric wire that directly contacts the pan-head of the pantograph and supplies electric power to the high-speed rail vehicle. Messenger wire is installed to support contact wire from above and keep overall stiffness uniform. A dropper is a cable that connects the contact wire to the messenger wire and maintains the contact wire at a fixed height. A moving bracket is a structure that stretches out from the electric pole, supports the messenger wire, and forms the beginning and the end of a span. A steady arm is installed to prevent uneven wear of contact wire and pan-head caused by partial contact and maintains a zigzag shape. Fig. 1 shows the structure of a simple catenary system.

2.1.2. Finite element analysis of the catenary system

Contact wire and messenger wire are modeled after a tensile beam to which constant tension is applied. A dropper, a moving bracket and a steady arm are modeled after a spring with a mass at each end. An analysis model structured for 10 spans of a catenary system can be expressed as shown in Fig. 2.

On the Gyeongbu high-speed railway, catenary systems with different characteristics are installed for different sections. The most conspicuous difference is span length which ranges from 38 to 63 m. The number of droppers for a span varies from 6 to 9 depending on the span length. In this study, four cases of representative span lengths, 40.5, 45, 49.5, and 63 m, are modeled and analyzed, respectively. We obtain Fig. 3 by expressing a finite element of contact wire and messenger wire and having it represent the degree of freedom

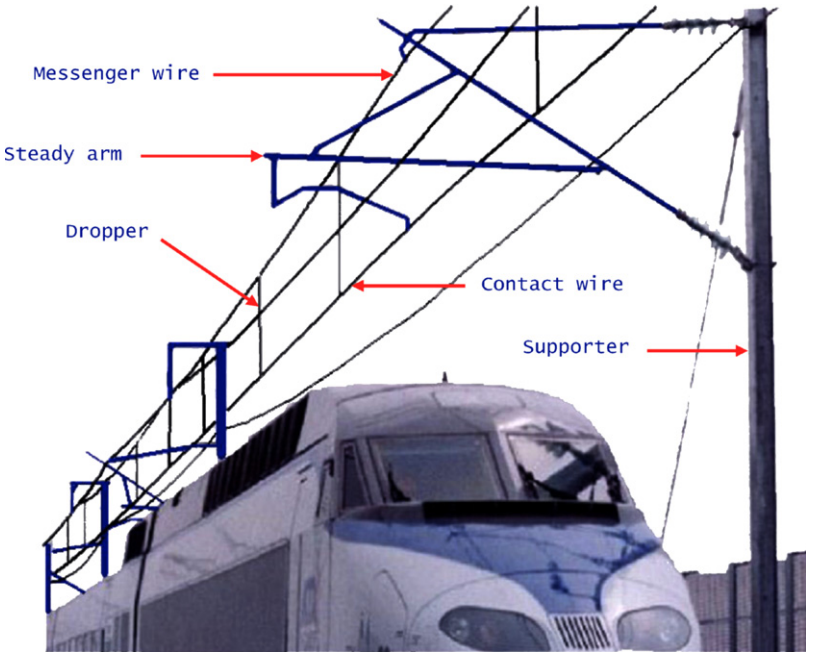

Fig. 1. The structure of a simple catenary system of a high-speed rail vehicle.

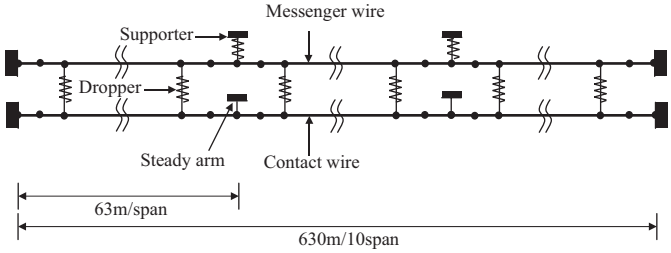

Fig. 2. Finite element model of 10 span catenary.

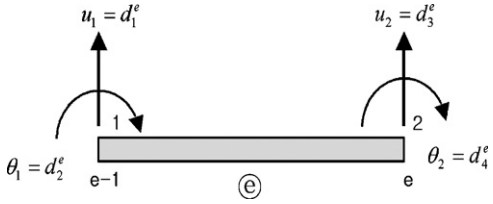

Fig. 3. Finite element of the wire.

at each nodal point. A beam is a long, slender structural member generally subjected to transverse loading that produces significant bending effects as opposed to twisting or axial effects. This bending deformation is represented as a transverse displacement and a rotation. Therefore, one element has 4 degree of freedom.

The stiffness matrix for a finite element of contact wire and messenger wire is as follows:

$$K_{\mathrm{ew}} = \frac{2EI}{h}\begin{bmatrix} \frac{6}{h^2} & \frac{3}{h} & \frac{-6}{h^2} & \frac{3}{h} \\ \frac{3}{h} & 2 & \frac{-3}{h} & 1 \\ \frac{-6}{h^2} & \frac{-3}{h} & \frac{6}{h^2} & \frac{-3}{h} \\ \frac{3}{h} & 1 & \frac{-3}{h} & 2 \end{bmatrix} + \frac{2T}{h}\begin{bmatrix} \frac{3}{5} & \frac{h}{20} & \frac{-3}{5} & \frac{h}{20} \\ \frac{h}{20} & \frac{h^2}{15} & \frac{-h}{20} & \frac{-h^2}{60} \\ \frac{-3}{5} & \frac{-h}{20} & \frac{3}{5} & \frac{-h}{20} \\ \frac{h}{20} & \frac{-h^2}{60} & \frac{-h}{20} & \frac{h^2}{15} \end{bmatrix}, \tag{1}$$

where h is the length of an element. Besides, the stiffness matrix for a finite element of droppers, moving brackets and steady arms is as follows:

$$K_{\mathrm{ed}} = \frac{k_d h}{5}\begin{bmatrix} \frac{13}{7} & \frac{11h}{42} & \frac{9}{14} & \frac{-13h}{84} \\ \frac{11h}{42} & \frac{h^2}{21} & \frac{13h}{84} & \frac{-h^2}{28} \\ \frac{9}{14} & \frac{13h}{84} & \frac{13}{7} & \frac{-11h}{42} \\ \frac{-13h}{84} & \frac{-h^2}{28} & \frac{-11h}{42} & \frac{h^2}{21} \end{bmatrix}, \tag{2}$$

$$K_{\mathrm{eb}} = \frac{k_b h}{5}\begin{bmatrix} \frac{13}{7} & \frac{11h}{42} & \frac{9}{14} & \frac{-13h}{84} \\ \frac{11h}{42} & \frac{h^2}{21} & \frac{13h}{84} & \frac{-h^2}{28} \\ \frac{9}{14} & \frac{13h}{84} & \frac{13}{7} & \frac{-11h}{42} \\ \frac{-13h}{84} & \frac{-h^2}{28} & \frac{-11h}{42} & \frac{h^2}{21} \end{bmatrix}, \tag{3}$$

$$K_{\mathrm{ea}} = \frac{k_a h}{5}\begin{bmatrix} \frac{13}{7} & \frac{11h}{42} & \frac{9}{14} & \frac{-13h}{84} \\ \frac{11h}{42} & \frac{h^2}{21} & \frac{13h}{84} & \frac{-h^2}{28} \\ \frac{9}{14} & \frac{13h}{84} & \frac{13}{7} & \frac{-11h}{42} \\ \frac{-13h}{84} & \frac{-h^2}{28} & \frac{-11h}{42} & \frac{h^2}{21} \end{bmatrix}. \tag{4}$$

The stiffness matrix for the whole catenary system is obtained from a combination of stiffness matrices for different elements:

$$K = \sum(K_{\mathrm{ew}}, K_{\mathrm{ed}}, K_{\mathrm{eb}}, K_{\mathrm{ea}}). \tag{5}$$

Now we will attempt to obtain the vertical-direction stiffness value following the position of a catenary system. The static equilibrium equation of a catenary system can be written as follows:

$$K\,\underline{d} = \underline{f}, \tag{6}$$

where $\underline{d}$ is the displacement vector of contact wire, and $\underline{f}$ the vector of external force applied to the contact wire. By arranging Eq. (6) for displacement vector, we get the following equation:

$$\underline{d} = K^{-1}\underline{f}. \tag{7}$$

From Eq. (7), we set the $\underline{f}$ vector in such a manner that a constant force is applied toward the vertical upper direction to a node on contact wire and calculate Eq. (7) to obtain the vertical upper-direction displacement at the node. We get the displacement vector of contact wire by repeating this procedure from the beginning to the end of a span. Here, by dividing the force f with the displacement vector, the upper-direction stiffness value at each node is obtained. This relationship can be expressed as Eq. (8):

$$\underline{k} = \frac{\underline{f}}{\underline{d}}. \tag{8}$$

From this, we get stiffness values at different positions of a span in a catenary system, and these values are periodically repeated following the adjacent span. Figs. 4–7 show stiffness values for a single span from those obtained for different span lengths, respectively.

In order to simulate the stiffness values following the position of the catenary system as previously obtained in conjunction with the pantograph, we can approximate as follows by expressing the stiffness values with a continuous equivalent function [5,13]:

$$K(x) = K_0\left(1 - \alpha\cos\frac{2\pi x}{L}\right), \tag{9}$$

$$K_0 = \frac{K_{\max} + K_{\min}}{2}, \tag{10}$$

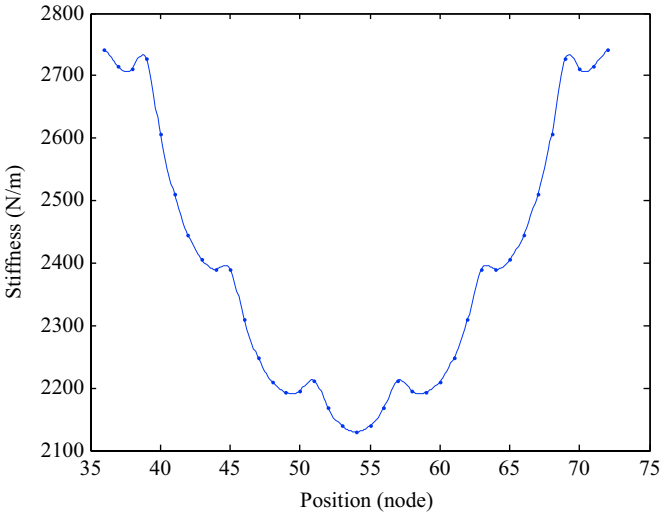

Fig. 4. Stiffness of the catenary (span length: 40.5 m).

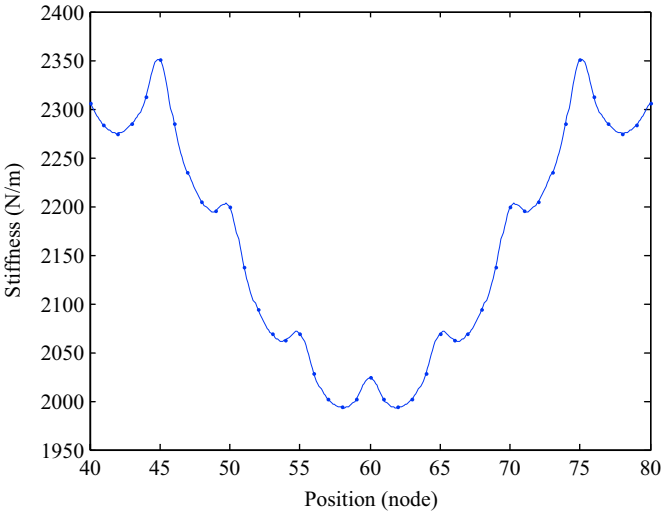

Fig. 5. Stiffness of the catenary (span length: 45 m).

$$\alpha = \frac{K_{\max} - K_{\min}}{K_{\max} + K_{\min}}, \tag{11}$$

where L is the the length of one span, $K_{\max}$ the largest stiffness in a span, $K_{\min}$ the smallest stiffness in a span.

When the pan-head contacts contact wire and moves at the speed of V, the stiffness value of the catenary system with respect to time t can be expressed as follows [5,13]:

$$K(t) = K_0\left(1 - \alpha \cos\frac{2\pi V}{L}t\right). \tag{12}$$

Using Eq. (9), the four types of stiffness values of the catenary system as previously analyzed can be expressed in Table 1. Fig. 8 is a graph that shows the equivalent functions of stiffness obtained here for a span, respectively.

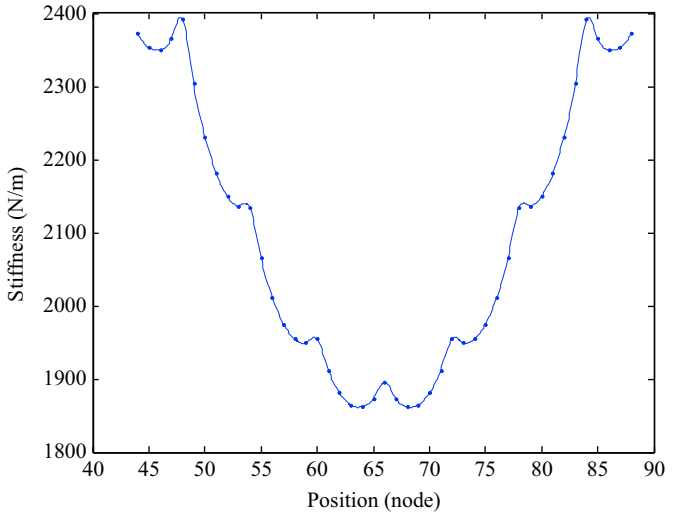

Fig. 6. Stiffness of the catenary (span length: 49.5 m).

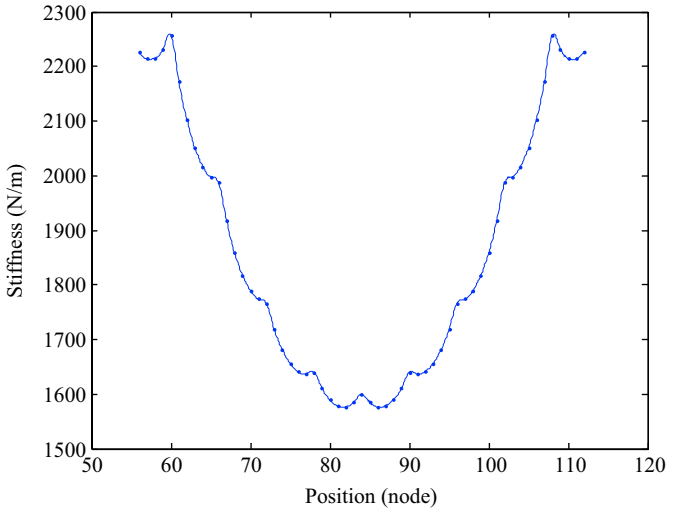

Fig. 7. Stiffness of the catenary (span length: 63 m).

Table 1
Equivalent function of the stiffness of each span

$L(m)$	K_0 (N/M)	α	$K(x)$
40.5	2435.6	0.1256	$2435.6\ (1-0.1256\cos 0.155x)$
45	2172	0.0823	$2172\ (1-0.0823\cos 0.14x)$
49.5	2126.6	0.1247	$2126.6\ (1-0.1247\cos 0.127x)$
63	1916.7	0.1776	$1916.7\ (1-0.1776\cos 0.1x)$

Such a stiffness function of a catenary system can be used for the analysis of a dynamic model for a pantograph system. In this way, the dynamic characteristics of a pantograph system can be realized more easily by realizing the behavior of a catenary system in a function.

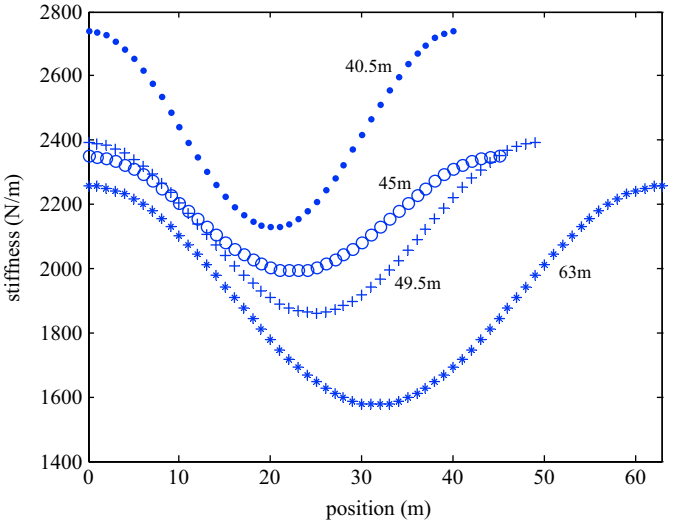

Fig. 8. Equivalent function of the catenary stiffness.

2.2. Modeling of the pantograph system

A pantograph system is a device that is installed on the roof of a power car running at a high speed of 350 km/h, takes electric power from the catenary, and supplies it to the main transformer of the power car. A pantograph for a high-speed rail vehicle requires analysis and design with air resistance that may occur during high-speed movement and other factors taken into consideration and needs to supply electric power stably by securing high-quality contact with contact wire. Besides, due to the causes vehicle vibration, change in external wind pressure, unevenness of elasticity on the catenary, stiffness variation at dropper connecting points, and others, temporary loss of contact between the catenary and the pantograph may take place. In preparation for such occasions, the pantograph system is designed to contact collection strips with the uplift force of about 70 N by an air piston.

In this thesis, we performed modeling and sensitivity analysis on grand Plongeur unique (GPU)-type pantographs installed on Korean-style high-speed rail vehicles. Its lower arm is connected to the base frame by a shaft and its upper arm connects from the upper end of the lower arm to the plunger. The cross bar is installed on the top of the plunger and supports the pan-head, which directly contacts the catenary and receives electric power. Fig. 9 shows the structure of a GPU pantograph system.

Fig. 10 shows the dynamic modeling from the GPU pantograph.

In Fig. 10, the pantograph model is composed of a 3-lumped mass, a spring, a damper, a friction damper between each mass, and the structure that supplies external force for each mass. The 3 dof pantograph modeling is defined in Fig. 10. The equations of motion are as follows:

$$m_3\ddot{y}_3 - c_3\dot{y}_2 - k_3y_2 + c_3\dot{y}_3 + k_3y_3 = F_3 + F_{L3} - F(t), \tag{13}$$

$$m_2\ddot{y}_2 - c_2\dot{y}_1 - k_2y_1 + (c_2 + c_3)\dot{y}_2 + (k_2 + k_3)y_2 - c_3\dot{y}_3 - k_3y_3 = F_2 + F_{L2}, \tag{14}$$

$$m_1\ddot{y}_1 + (c_1 + c_2)\dot{y}_1 + (k_1 + k_2)y_1 - c_2\dot{y}_2 - k_2y_2 = F_1 + F_{L1}, \tag{15}$$

where F_1, F_2 and F_3 are static uplift forces. Also, F_{L1}, F_{L2} and F_{L3} means the lift force. $F(t)$ means the contact force occurring in between the contact wire and the pantograph pan-head. The contact force is one of the most important thing in analyzing dynamic characteristic of the catenary-pantograph system. It is related to displacement of pan-head directly. From Eq. (12), the contact force is derived from the stiffness of the

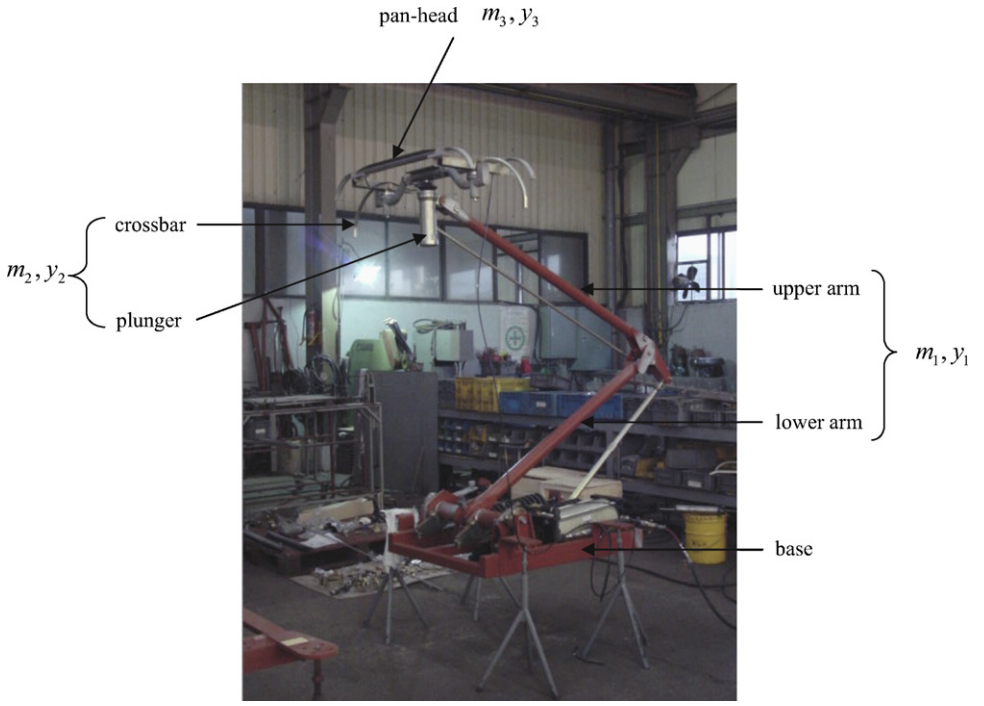

Fig. 9. GPU type pantograph.

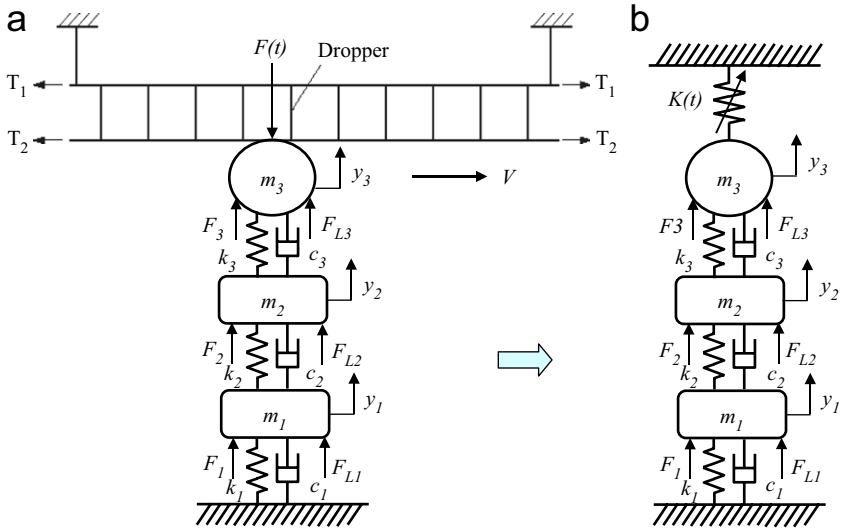

Fig. 10. Dynamic modeling of the pantograph.

catenary system only. Using Eq. (12) the contact force is as follows:

$$F(t) = K(t)y_3 = K_0\left(1 - \alpha\cos\frac{2\pi V}{L}t\right)y_3. \tag{16}$$

Eq. (16) calculates contact force by varying as vehicle velocity changes. The contact force is also affected by y_3 from the catenary stiffness function. Eq. (13) is modified as follows:

$$m_3\ddot{y}_3 - c_3\dot{y}_2 - k_3y_2 + c_3\dot{y}_3 + (k_3 + K(t))y_3 = F_3 + F_{L3}. \tag{17}$$

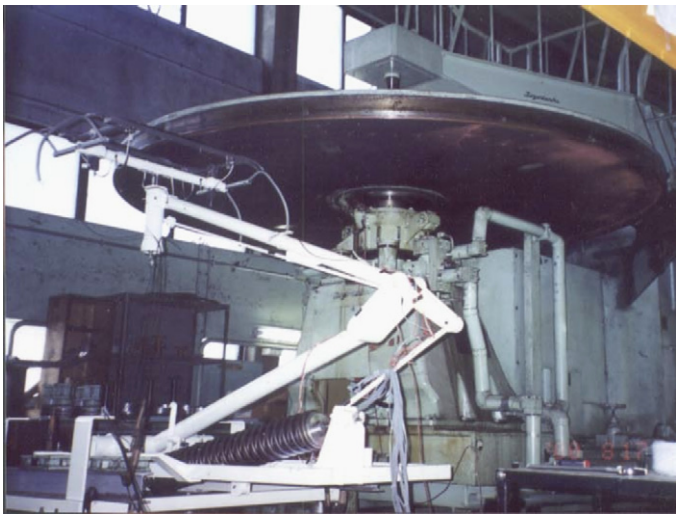

Fig. 11. Pantograph vibration experiment.

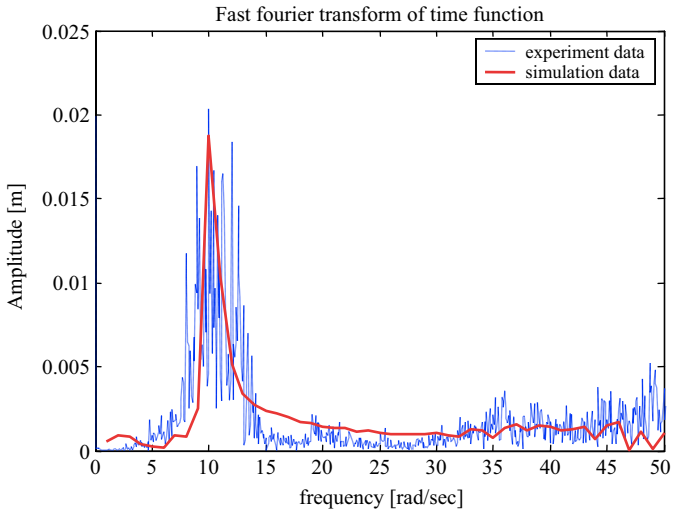

Fig. 12. Comparison to experimental data and simulation data *experiment* (- - -) and *modelling* (—).

2.3. *Verification of pantograph modeling*

Fig. 11 shows the vibration experiment equipment which is mounted on the pantograph. The large disk has a wave pattern through its radial direction and is driven to rotate in the contact condition with pan-head. The more the rotating velocity of the large wavelet disk increases, the higher the input frequency of pan-head is. Hence, continuous increase of rotating speed in the wavelet disk means sine sweep input to the pantograph. The response of the pantograph to sine sweep input is measured through accelerometers in time function. Because the acquired data is vibrational signal in linearly accelerated rotating speed, the magnitude per rotating speed (frequency) of time function corresponds to magnitude per frequency of FFT.

Fig. 12 shows the result that compares the actual data of the excitation experiment with the simulation data. As a result of simulation indicates, the natural frequency on the system is at the level of 10 rad/s.

That is significantly similar to the actual experimental result. Therefore, it is deemed to confirm the propriety of linear 3 dof modeling on the pantograph that was proposed earlier.

2.4. The effect of aerodynamic lift force

The high-speed rail vehicle runs at a high speed of up to 350 km/h and, in this case, there may be several aerodynamic problems caused by the high speed. Therefore, the aerodynamic design of pantograph is very important in order to secure stable collection capability. As the speed of the train increases under the pantograph for a high-speed rail vehicle, the uplift force and noise increase as well due to the lift force. When the aerodynamic lift force occurs, the part that is affected the most is the pan-head and, depending on the formation, the uplift coefficient of both phases differs, while the noise is affected as well. Recently, a wind tunnel test was performed in order to estimate the characteristics of the lift force and noise with a pantograph system for a high-speed rail vehicle [14]. For measuring the aerodynamic lift force, the wind speed was performed under 5 conditions (150, 200, 250, 300, and 350 km/h). Fig. 13 shows the result of fitting in quadratic function for the aerodynamic lift force in speed to check the lift force coefficient.

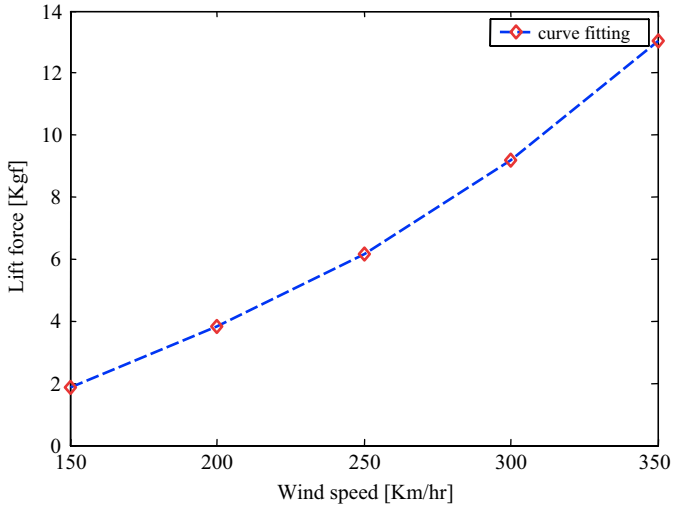

Fig. 13. The relation between wind speed and lift force.

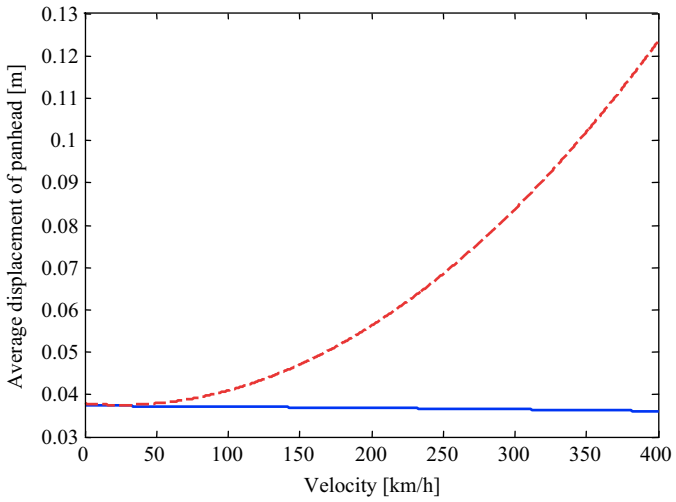

Fig. 14. Average displacement of pan-head.

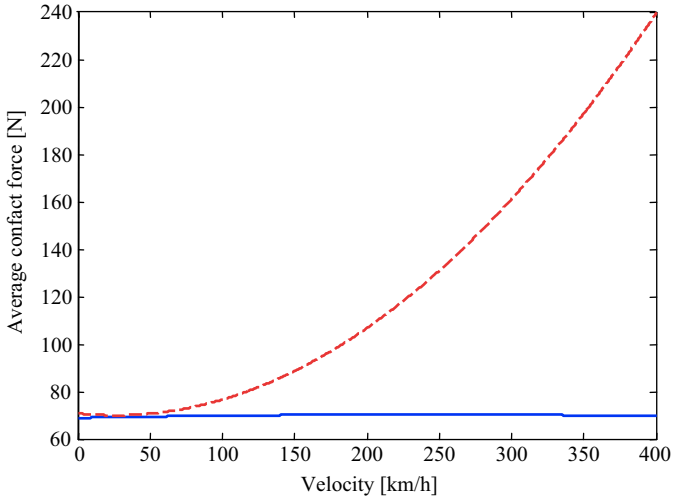

Fig. 15. Average contact force between the catenary and the pantograph.

In general, the lift force and the wind speed are in a functional relationship, and may be expressed in the following Eq. (18):

$$F_{L3} = (1.26554 \times 10^{-4})x^2 - 0.00769x + 0.19851. \tag{18}$$

In Eq. (18), F_{L3} means the lift force (kgf) operating to pan-head, x means the wind speed (km/h), respectively. It can be obtained from Fig. 13. A simulation is made for the displacement and contact force of the pan-head in terms of consideration given for lift force in Figs. 14 and 15 and the case of consideration not given. As shown in Figs. 14 and 15, if the lift force is not considered, the displacement and contact force of the pan-head shows almost consistent response, but if the aerodynamic lift force is considered, the displacement and contact force of the pan-head is gradually increasing in the quadratic function form following the speed increase. As such, the increase of uplift force by the lift force directly affect the displacement and contact force occurring in between the catenary and the pantograph. So, in the event of performing the dynamic analysis, it necessarily has to be considered.

3. State sensitivity analysis

The sensitivity analysis of the vibration system shows how much the design variable of the system affect the vibration characteristics including displacement, speed, acceleration and the like. In addition, the size of sensitivity displays the degree of sensitivity of design variables of structure to the required condition. In this paper, the direct differentiation method is used to perform the sensitivity analysis [14]. Also, design variables composed the pantograph system and a span length and static uplift force was regarded as all design variables. By contemplating the factors that affect the displacement of the pan-head that arises when operating the high-speed rail vehicle, it has a basis on the selection of design variable to minimize the vibration occurring in between the catenary and the pantograph.

3.1. Sensitivity formulation

In order to perform sensitivity analysis, state sensitivity equations must be derived with respect to the design variables at the initial stage. In this study, the state variables of the system are as follows:

$$\mathbf{z} = [y_1 \quad \dot{y}_1 \quad y_2 \quad \dot{y}_2 \quad y_3 \quad \dot{y}_3]^{\mathrm{T}}, \tag{19}$$

where $\mathbf{z}$ is the state variable vector, y and $\dot{y}$ are displacements and velocities of each mass, respectively. Design variables of this system are selected to be the following:

$$\begin{aligned}\mathbf{b} &= [b_1 \quad b_2 \quad b_3 \quad b_4 \quad b_5 \quad b_6 \quad b_7 \quad b_8]^{\mathrm{T}} \\ &= [m_1 \quad m_2 \quad m_3 \quad c_1 \quad k_2 \quad k_3 \quad F_1 \quad L]^{\mathrm{T}}.\end{aligned} \tag{20}$$

The dynamic equations of motion for the pantograph system can be expressed in the following form:

$$\dot{\mathbf{z}} = \begin{bmatrix} \dot{y}_1 \\ \frac{1}{m_1}\{-(k_1+k_2)y_1 - (c_1+c_2)\dot{y}_1 + k_2 y_2 + c_2\dot{y}_2 + F_1 + F_{L1}\} \\ \dot{y}_2 \\ \frac{1}{m_2}\{k_2 y_1 + c_2\dot{y}_1 - (k_2+k_3)y_2 - (c_2+c_3)\dot{y}_2 + k_3 y_3 + c_3\dot{y}_3 + F_2 + F_{L2}\} \\ \dot{y}_3 \\ \frac{1}{m_3}\{k_3 y_2 + c_3\dot{y}_2 - (k_3+k(t))y_3 - c_3\dot{y}_3 + F_3 + F_{L3}\} \end{bmatrix}. \tag{21}$$

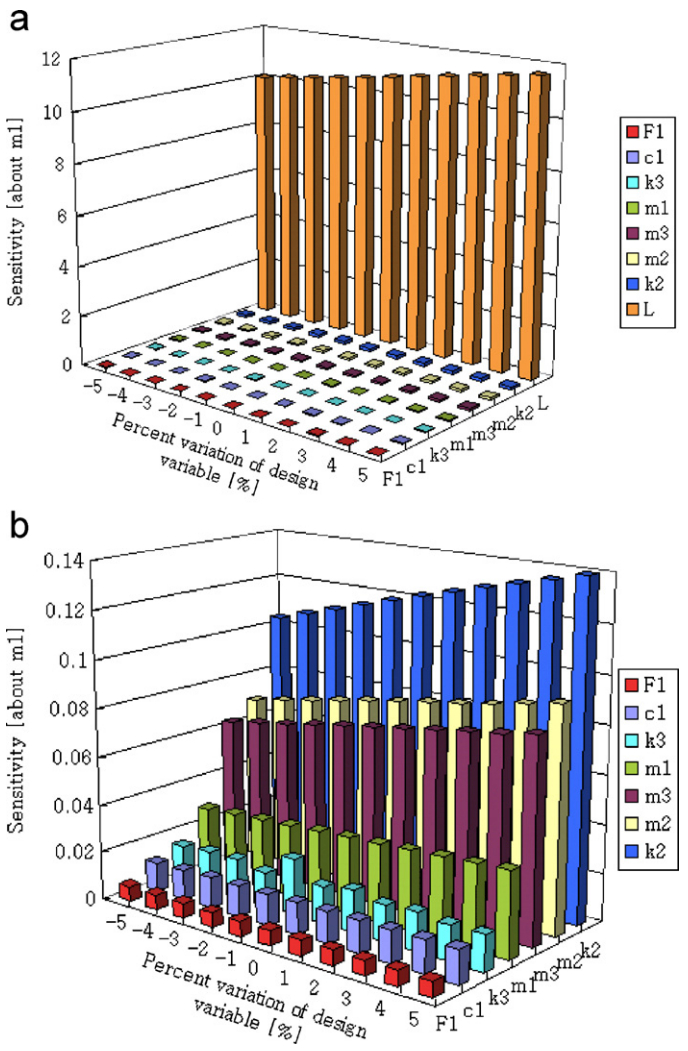

Fig. 16. The result of sensitivity analysis (about m_1): (a) sensitivity results; (b) sensitivity results except design variable L.

This equation has the form of a first-order ordinary differential equation. In order to perform sensitivity analysis, state sensitivity equations must be derived with respect to the design variables at the initial stage. A general form of the first order differential sensitivity equations is

$$\frac{\partial \dot{\mathbf{z}}}{\partial \mathbf{b}} = \frac{\partial \mathbf{f}}{\partial \mathbf{z}} \cdot \frac{\mathrm{d}\mathbf{z}}{\mathrm{d}\mathbf{b}} + \frac{\partial \mathbf{f}}{\partial \mathbf{b}}. \tag{22}$$

This equation can be written in the following compact matrix form:

$$\dot{\mathbf{z}}_b = \mathbf{f}_z \cdot \mathbf{z}_b + \mathbf{f}_b, \tag{23}$$

where $\mathbf{z} \in \mathbf{R}^n$, $\mathbf{b} \in \mathbf{R}^n$, $\mathbf{f} \in \mathbf{R}^n$, $\mathbf{z} \in \mathbf{R}^{n\times m}$, $\mathbf{f}_z \in \mathbf{R}^{n\times n}$, and $\mathbf{f}_b \in \mathbf{R}^{n\times m}$. n is the number of state variables and m is the number of design variables. In this case, n is 6 and m is 8 from Eq. (21). $\mathbf{z}_b$ is state sensitivity matrix with respect to the design variables and $\dot{\mathbf{z}}_b$ is the time derivative of the state sensitivity matrix. For linear differential equations, $\mathbf{f}_z$ can be expressed by system matrix A. From this idea, Eq. (23) can be re-written in the following form:

$$\dot{\mathbf{z}}_b = \mathbf{A} \cdot \mathbf{z}_b + \mathbf{f}_b. \tag{24}$$

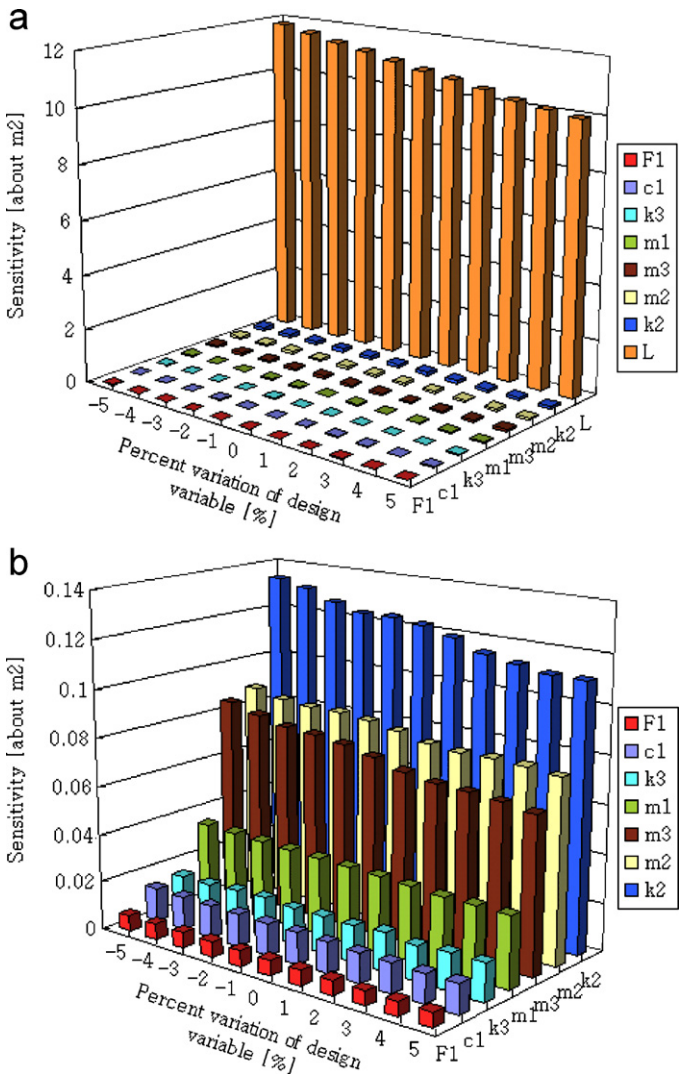

Fig. 17. The result of sensitivity analysis (about m_2): (a) sensitivity results; (b) sensitivity results except design variable L.

The system matrix A is expressed as follows:

$$A = \begin{bmatrix} 0 & 1 & 0 & 0 & 0 & 0 \\ -\dfrac{k_1+k_2}{m_1} & -\dfrac{c_1+c_2}{m_1} & \dfrac{k_2}{m_1} & \dfrac{c_2}{m_1} & 0 & 0 \\ 0 & 0 & 0 & 1 & 0 & 0 \\ \dfrac{k_2}{m_2} & \dfrac{c_2}{m_2} & -\dfrac{k_2+k_3}{m_2} & -\dfrac{c_2+c_3}{m_2} & \dfrac{k_3}{m_2} & \dfrac{c_3}{m_2} \\ 0 & 0 & 0 & 0 & 0 & 1 \\ 0 & 0 & \dfrac{k_3}{m_3} & \dfrac{c_3}{m_3} & -\dfrac{k_3+k(t)}{m_3} & -\dfrac{c_3}{m_3} \end{bmatrix}. \tag{25}$$

Next, $\mathbf{f}_b$ should be obtained from the last term of the state sensitivity analysis with respect to the design variables; this term is expressed in the following matrix form:

$$\mathbf{f}_b = [\mathbf{f}_{b1}, \mathbf{f}_{b2}, \mathbf{f}_{b3}, \mathbf{f}_{b4}, \mathbf{f}_{b5}, \mathbf{f}_{b6}, \mathbf{f}_{b7}, \mathbf{f}_{b8}]_{6\times 8}. \tag{26}$$

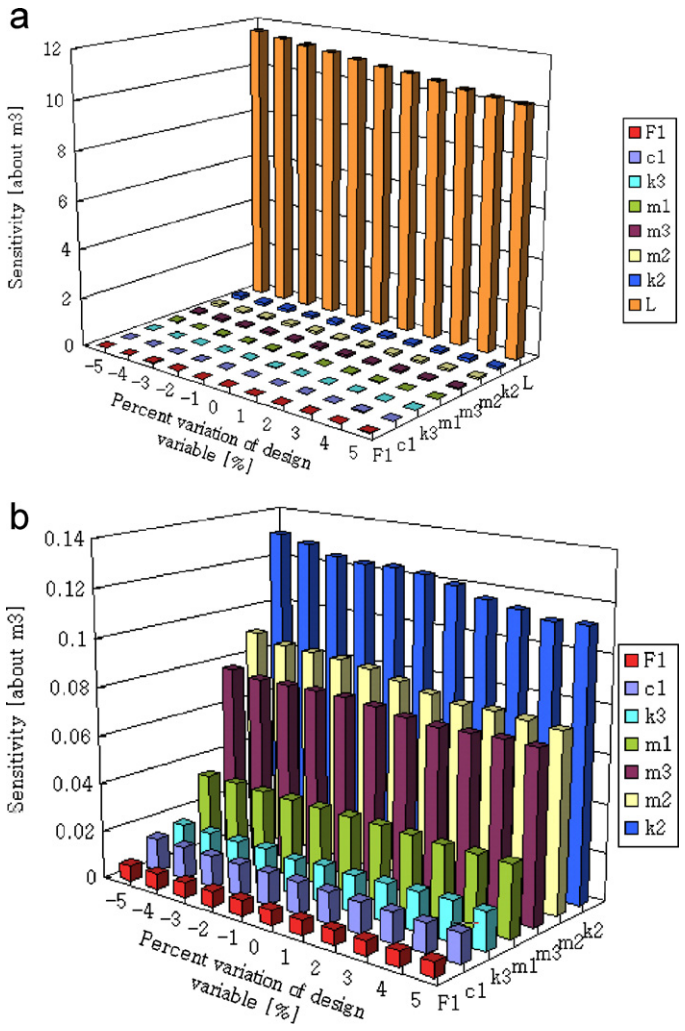

Fig. 18. The result of sensitivity analysis (about m_3): (a) sensitivity results; (b) sensitivity results except design variable L.

Detailed derivations of the above are summarized in the appendix. In order to solve the dynamic and state sensitivity equations of the system, Eqs. (21) and (24) are simultaneously integrated [15].

3.2. The result of sensitivity analysis

From the design variables c_2, c_3 and k_1 values were all 0 that they were excluded from the sensitivity analysis. The running speed of pantograph started from 0 s to increase consistently with the time to reach 100 s at the highest speed of 400 km/h for a simulation. After calculating the sensitivity value for each speed on the displacement of the pan-head, the difference of the maximum value and the minimum value are calculated. Also, for the reliability of the sensitivity analysis result, the guaranty of linearity in each design variable range has to be confirmed. Figs. 16–23 calculated the sensitivity on the displacement of pan-head by actually changing each design variable for −5%–+5%. This result is presumed with the perturbation of 1% for each design variable and is a result obtained through the normalizing process. We could show that the result of

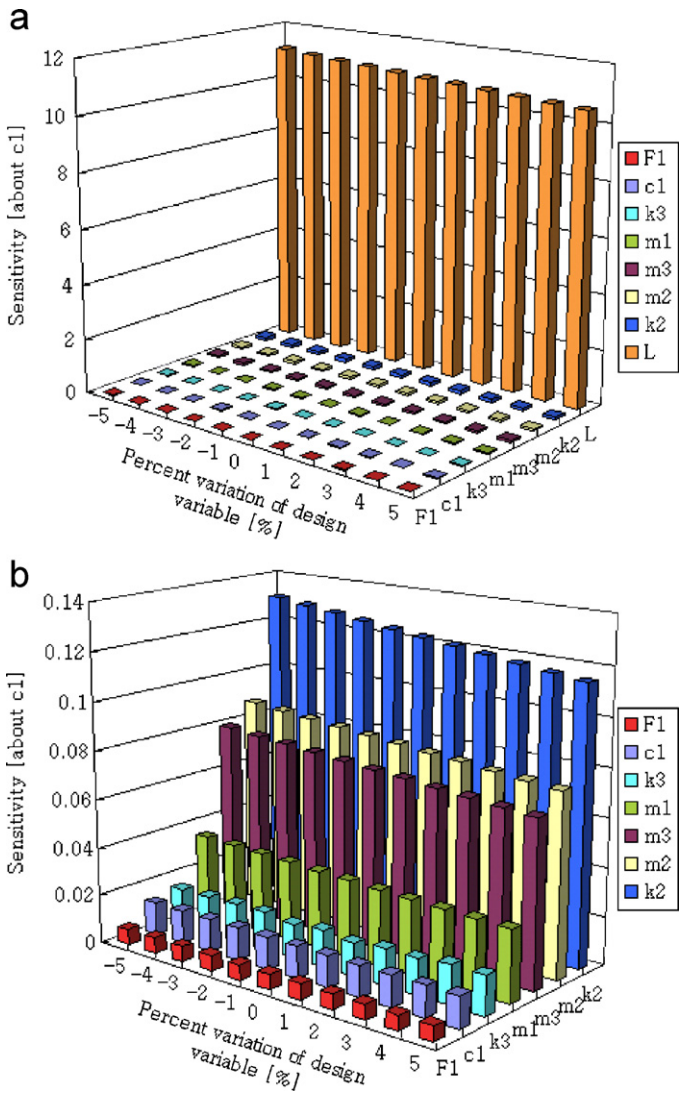

Fig. 19. The result of sensitivity analysis (about c_1): (a) sensitivity results; (b) sensitivity results except design variable L.

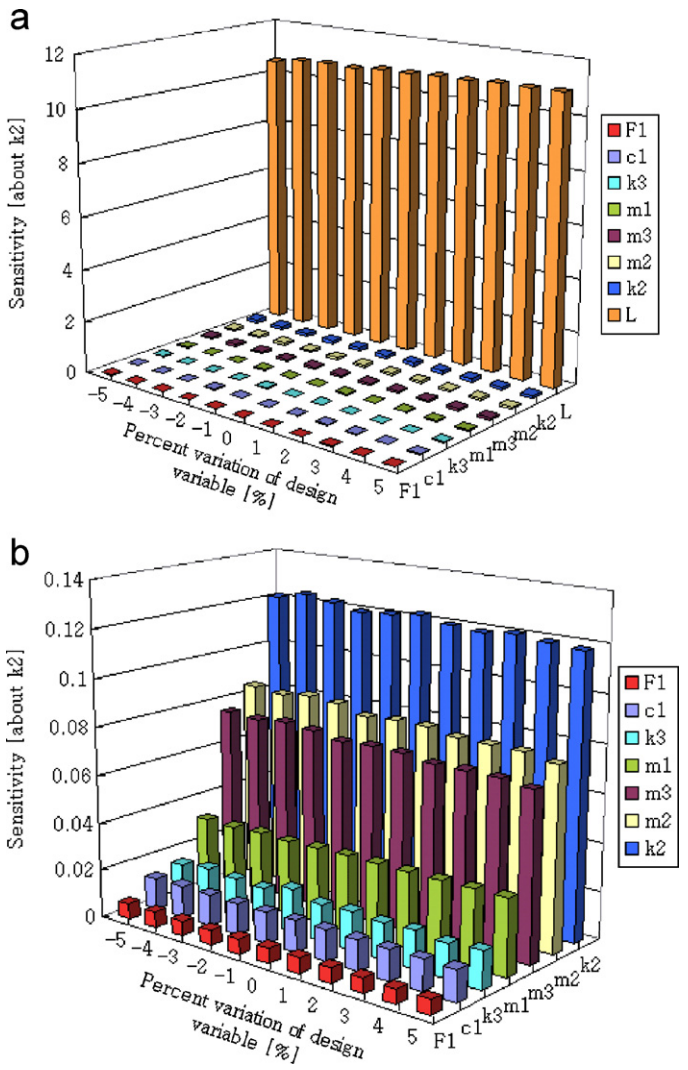

Fig. 20. The result of sensitivity analysis (about k_2): (a) sensitivity results; (b) sensitivity results except design variable L.

the sensitivity analysis can be relied upon within the -5%–$+5\%$ range on the given design variable. In Figs. 16–23, (a) show the sensitivity about all design variables and (b) show the sensitivity about the rest design variables except design variable L. As a result of sensitivity analysis, the sensitivity on the displacement of pantograph pan-head showed the greatest value on the span length L. This means that the factor that affects the greatest in the displacement of pantograph pan-head at high-speed runs is the span length. In design variables composed the pantograph system, the sensitivity on the displacement of pantograph pan-head showed the greatest value on the plunger spring constant k_2. From the sensitivity analysis, we could confirm that the displacement of pantograph pan-head is much more sensitive not so much design variables composed the pantograph system as a span length.

3.3. *Verification of simulation result*

In this paper, the purpose is to study the factors that most affect the pan-head of the pantograph during the operation of a high-speed rail vehicle and select the optimal design variable. As a result of sensitivity analysis,

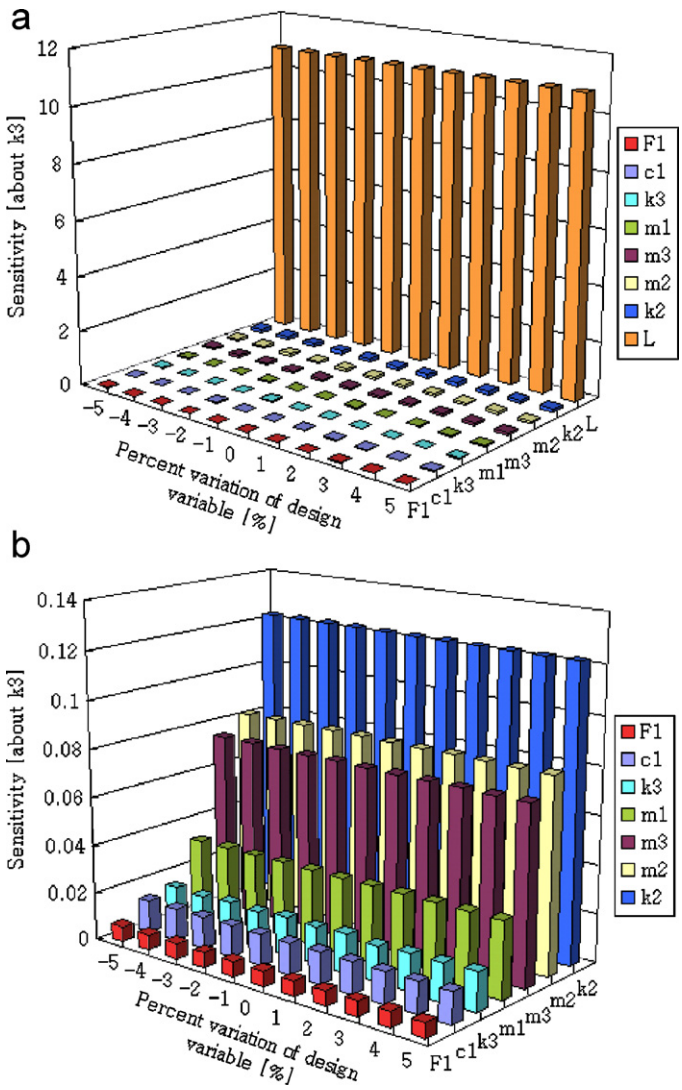

Fig. 21. The result of sensitivity analysis (about k_3): (a) sensitivity results; (b) sensitivity results except design variable L.

the span length (L) and the plunger spring constant (k_2) are confirmed as the most sensitive design variables for the pan-head displacement. Based on this result, when the design variable of each is actually changed for $-5\%-+5\%$, the range of width of displacement occurring in the pan-head is shown in Fig. 24. As shown in Fig. 20, when the span length (L) and the plunger spring constant (k_2) were changed for $-5\%-+5\%$, the change of the pan-head displacement was the greatest, and this is very consistent to the result of the sensitivity analysis performed earlier.

4. Conclusions

In this paper, dynamic characteristics analysis of a catenary-pantograph system is performed. The catenary system is analyzed by FEM. The contact and the messenger wire were modeled as beams with bending stiffness and tension. Displacement of pan-head is the main factor for dynamic performance of pantograph, and it is

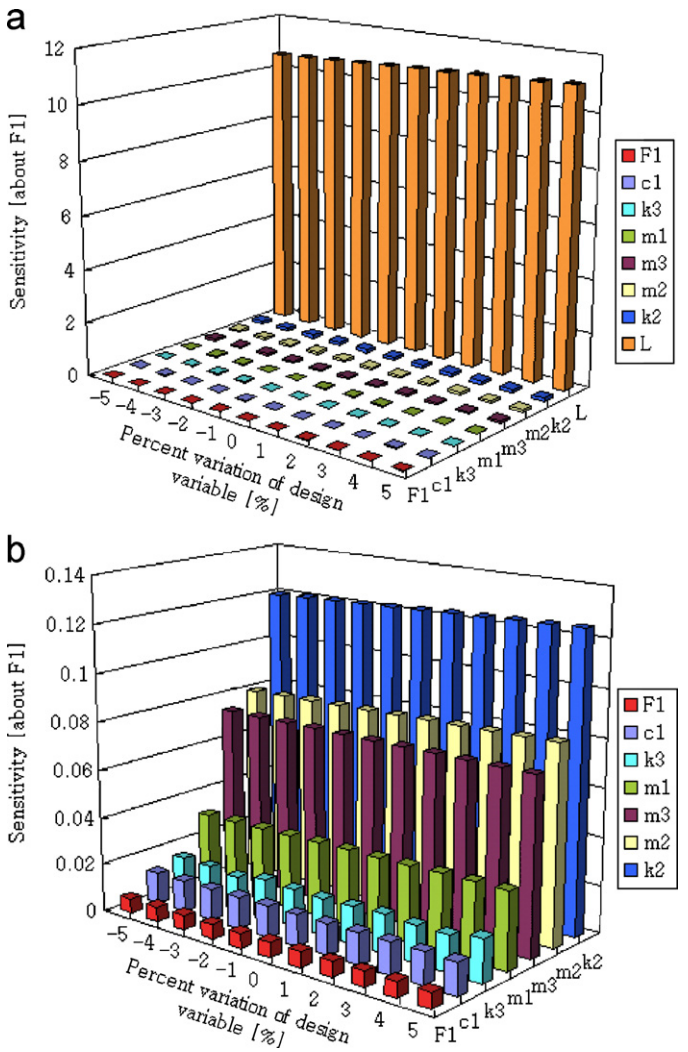

Fig. 22. The result of sensitivity analysis (about F_1): (a) sensitivity results; (b) sensitivity results except design variable L.

related to contact force directly. So design variables that are related to vibration characteristics of pantograph through sensitivity information are discussed.

The conclusions of this paper are as follows:

1. Using the FEM, stiffness value according to position of contact line in 1 span was calculated and this approximated as periodic functions.
2. 3 dof pantograph modeling is verified by experimental data obtained through vibration experiments and confirmed that natural frequency of the catenary-pantograph system is at the level of 10 rad/s.
3. As a result of sensitivity analysis, we now know that dominant design variables related to dynamic characteristics of the catenary-pantograph system are a span length L and plunger spring constant k_2.
4. To minimize dynamic motion occurring at high-speed runs, the pantograph system insensibility to a span length and aerodynamic lift force effect need to develop.

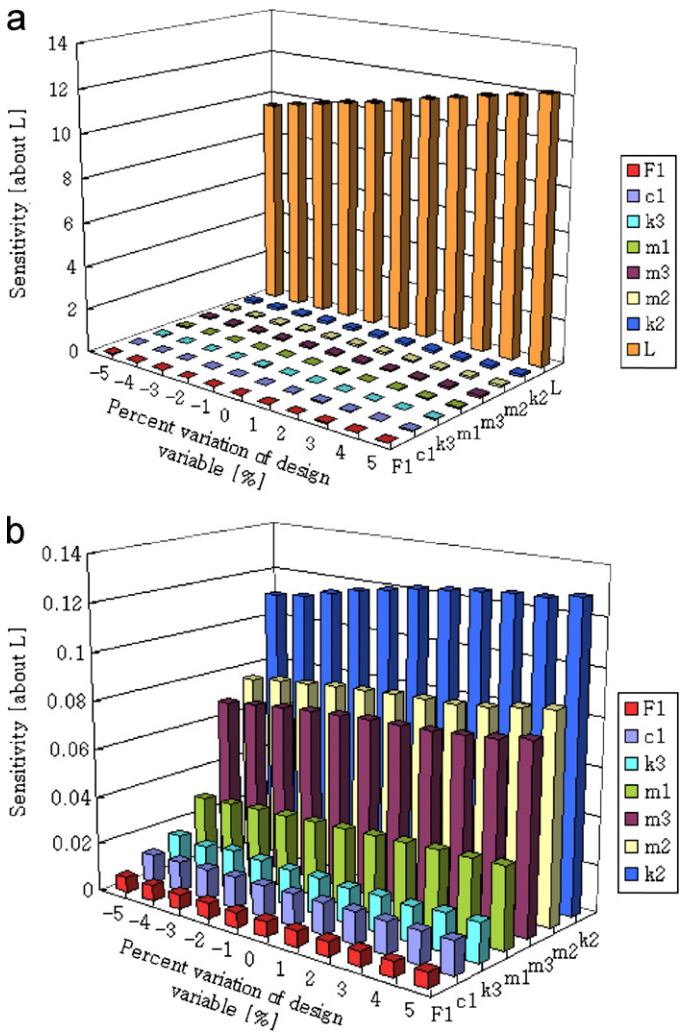

Fig. 23. The result of sensitivity analysis (about L): (a) sensitivity results; (b) sensitivity results except design variable L.

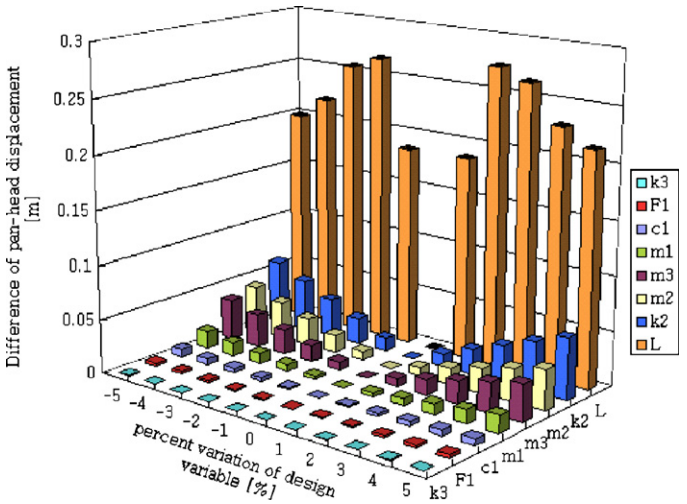

Fig. 24. Difference of pan-head displacement about percent variation of design variables.

Appendix A

A.1. Sensitivity formulations

Sensitivity functions for RHS terms of Eq. (26) are derived as follows with nine sensitivity equations for each design variable obtained from partial derivative operation with respect to design variables.

(1) For $b_1 = m_1$

$$\mathbf{f}_{b_1} = \begin{bmatrix} 0 \\ -\frac{1}{m_1^2}\{-(k_1+k_2)z_1 - (c_1+c_2)z_2 + k_2 z_3 + c_2 z_4 + F_1 + F_{L1}\} \\ 0 \\ 0 \\ 0 \\ 0 \end{bmatrix}. \tag{A.1}$$

(2) For $b_2 = m_2$

$$\mathbf{f}_{b_2} = \begin{bmatrix} 0 \\ 0 \\ 0 \\ -\frac{1}{m_2^2}\{k_2 z_1 + c_2 z_2 - (k_2+k_3)z_3 - (c_2+c_3)z_4 + k_3 z_5 + c_3 z_6 + F_2 + F_{L2}\} \\ 0 \\ 0 \end{bmatrix}. \tag{A.2}$$

(3) For $b_3 = m_3$

$$\mathbf{f}_{b_3} = \begin{bmatrix} 0 \\ 0 \\ 0 \\ 0 \\ 0 \\ -\frac{1}{m_3^2}\{k_3 z_3 + c_3 z_4 - (k_3 + k(t))z_5 - c_3 z_6 + F_3 + F_{L3}\} \end{bmatrix}. \tag{A.3}$$

(4) For $b_4 = c_1$

$$\mathbf{f}_{b_4} = \begin{bmatrix} 0 \\ -\frac{z_2}{m_1} \\ 0 \\ 0 \\ 0 \\ 0 \end{bmatrix}. \tag{A.4}$$

(5) For $b_5 = k_2$

$$\mathbf{f}_{b_5} = \begin{bmatrix} 0 \\ -\dfrac{z_1}{m_1} + \dfrac{z_3}{m_1} \\ 0 \\ \dfrac{z_1}{m_2} - \dfrac{z_3}{m_2} \\ 0 \\ 0 \end{bmatrix} \quad Mbdeno; \tag{A.5}$$

(6) For $b_6 = k_3$

$$\mathbf{f}_{b6} = \begin{bmatrix} 0 \\ 0 \\ 0 \\ -\dfrac{z_3}{m_2} + \dfrac{z_5}{m_2} \\ 0 \\ \dfrac{z_3}{m_3} - \dfrac{z_5}{m_3} \end{bmatrix}. \tag{A.6}$$

(7) For $b_7 = F_1$

$$\mathbf{f}_{b7} = \begin{bmatrix} 0 \\ \dfrac{1}{m_1} \\ 0 \\ 0 \\ 0 \\ 0 \end{bmatrix}. \tag{A.7}$$

(8) For $b_8 = L$

$$\mathbf{f}_{b8} = \begin{bmatrix} 0 \\ 0 \\ 0 \\ 0 \\ 0 \\ \dfrac{1}{m_3}\left\{\alpha \cos\dfrac{2\pi V}{L} t\left(2\pi V \dfrac{1}{L^2}\right)\right\} z_5 \end{bmatrix}. \tag{A.8}$$

References

[1] J.R. Ockendon, A.B. Tayor, The dynamics of a current collection system for an electric locomotive, *Proceedings of the Royal Society of London A* 211 (1971) 336–357.

[2] C.N. Jensen, H. True, S. Consult, Dynamic of an electrical overhead line system and moving pantographs, *Vehicle System Dynamic* 28 (1998) 104–113.

[3] E.J. Haug, V.N. Sohoni, Design sensitivity analysis and optimization of kinematically driven systems, *Computer Aided Analysis and Optimization of Mechanical System Dynamics, NATO ASI Series F: Computer and System Sciences*, Vol. 9, 1994, pp. 499–554.

[4] K. Manabe, Periodical dynamic stabilities of a catenary-pantograph system, *QR of RTRI*, Vol. 35, 1994, pp. 112–117.

[5] T.X. Wu, M.J. Brennan, Basic analytical study of pantograph-catenary system dynamics, *Vehicle System Dynamic* 30 (1998) 443–456.
[6] T. Vinayagalingam, Computer evaluation of controlled pantographs for current collection from simple catenary overhead equipment at high speed, *ASME Journal of Dynamics Systems Measurement and Control* 105 (1983) 287–294.
[7] A. Balestrino, O. Bruno, A. Landi, L. Sani, Innovative solutions for overhead catenary-pantograph system: wire actuated control and observed contact force, *Vehicle System Dynamic* 33 (2000) 69–89.
[8] D.N. O'Connor, S.D. Eppinger, W.P. Seering, D.N. Wormley, Active control of a high-speed pantograph, *Journal of Dynamic Systems, Measurement, and Control* 119 (1997) 1–4.
[9] G. Diana, F. Fossati, F. Resta, High speed railway: collecting pantographs active control and overhead lines diagnostic solutions, *Vehicle System Dynamic* 30 (1998) 69–84.
[10] C.N. Vanderplaats, *Numerical Optimization Techniques for Engineering Design with Applications*, McGraw-Hill, New York, 1984.
[11] J.S. Arora, *Introduction to Optimum Design*, McGraw-Hill, New York, 1989.
[12] J.H. Jang, C.S. Han, The state sensitivity analysis of the front wheel steering vehicle: in the time domain, *KSME International Journal* 11 (1997) 595–604.
[13] T.X. Wu, M.J. Brennan, Dynamic stiffness of a railway overhead wire system and its effect on pantograph-catenary system dynamics, *Journal of Sound and Vibration* 219 (1999) 483–502.
[14] A.S. Deif, *Sensitivity Analysis in Linear System*, Springer, Berlin, Heidelberg, 1986.
[15] M. Eslami, *Theory of Sensitivity in Dynamic System*, Springer, Berlin, Heidelberg, 1994.